JCTC Journal of Chemical Theory and Computation

Monte Carlo Simulations of an Isolated *n*-Octadecane Chain Solvated in Water−Acetonitrile Mixtures

Li Sun,[†] J. Ilja Siepmann,*[,†] and Mark R. Schure[‡]

Departments of Chemistry and of Chemical Engineering and Materials Science, University of Minnesota, 207 Pleasant Street SE, Minneapolis, Minnesota 55455, and Theoretical Separation Science Laboratory, Rohm and Haas Company, 727 Norristown Road, P.O. Box 0904, Spring House, Pennsylvania 19477

Received July 21, 2006

Abstract: To investigate conformational properties of an isolated *n*-octadecane chain solvated in water−acetonitrile mixtures, configurational-bias Monte Carlo simulations in the isobaric−isothermal ensemble were performed at $T = 323$ K and $p = 10$ atm. The united-atom version of the transferable potentials for phase equilibria force field was used to represent *n*-octadecane and acetonitrile, and the TIP-4P model was used for water. In all four environments (neat water, 33 and 67 mole percent acetonitrile, and neat acetonitrile), similar conformational distributions are observed as in a previous study for water−methanol solvent mixtures; that is, the *n*-octadecane chain is found to predominantly adopt extended but not all-trans conformations, and only a small fraction of more collapsed conformations is observed for aqueous hydration, water-rich solvent environments. Analysis of the local solvation structures in the water−acetonitrile mixtures shows an enrichment of the acetonitrile molecules near the methylene and methyl segments of the *n*-octadecane chain. However, upon increasing the concentration of acetonitrile, the enhancement of acetonitrile and the depletion of water is more pronounced than for water−methanol mixtures because of the weaker interactions between acetonitrile and water.

1. Introduction

Water−acetonitrile and water−methanol mixtures are the most commonly used mobile phases in reversed-phase liquid chromatography (RPLC). When the fraction of organic modifier in the mobile phase falls below a certain threshold, a loss of retention is usually observed. It was suggested that the retention loss is due to the collapse of alkyl chains in the stationary phase.[1,2] It was also observed that some solutes have different thermodynamic behavior in the two different mobile phases,[3−5] and the formation of acetonitrile pockets in the organic-rich mobile phase was suggested to be a very important factor.[3,4,6,7] Isotherm measurements show that acetonitrile forms a much thicker adsorbed layer (with dimensions of four to five molecules) near the hydrophobic surface of the RPLC bonded phase than that observed for methanol (only a monolayer), and retention can occur in the interfacial environment.[8]

Particle-based molecular simulations have also been applied to study water−acetonitrile mixtures.[9−12] It was found that the water structure is enhanced upon adding acetonitrile, whereas the acetonitrile structure remains relatively intact in the aqueous solution.[9] Other simulations point to a broad size distribution for water clustering that fills in the spaces naturally occurring in the acetonitrile liquid. However, the clustering is not thought to be an important feature influencing retention; the properties of long chain molecules are considered to be more important.[10,11] Some molecular dynamics studies of simplified RPLC model systems with C_8 or C_{18} chains as a stationary phase yield a picture with the chains densely packed near the substrate and little solvent penetration.[13,14] In contrast, recent simulations for RPLC

* Corresponding author fax: (612) 626-7541; e-mail: siepmann@chem.umn.edu.
[†] University of Minnesota.
[‡] Rohm and Haas Co.

10.1021/ct600239z CCC: $37.00
Published on Web 01/05/2007

Table 1. Simulation Details and Ensemble Averages: Numbers of *n*-Octadecane and Solvent Molecules, Number of Monte Carlo Production Cycles for Each Independent Simulation, Average Linear Dimension of the Simulation Box (in Units of Å), Average End-to-End Length (in Units of Å), and Folding Equilibrium Constant for Comparison[a]

system	N (C_{18})	N (H_2O)	N (ACN/MeOH)	N_{MC}	$\langle L \rangle$	$\langle r_E \rangle$	$\langle K_{UN} \rangle$
WAT	1	900		2.3×10^5	30.40 ± 0.06	14.8 ± 0.4	0.11 ± 0.03
33A	1	600	300	2.7×10^5	35.83 ± 0.02	14.7 ± 0.8	0.10 ± 0.03
67A	1	300	600	2.6×10^5	40.01 ± 0.01	15.3 ± 0.2	0.027 ± 0.008
ACN	1		900	2.3×10^5	43.47 ± 0.01	15.6 ± 0.2	0.032 ± 0.012
33M	1	600	300	3.4×10^5	33.94 ± 0.06	14.1 ± 0.3	0.13 ± 0.03
67M	1	300	600	3.2×10^5	37.05 ± 0.07	15.4 ± 0.2	0.035 ± 0.03
MET	1		900	3.5×10^5	39.94 ± 0.07	16.1 ± 0.2	0.013 ± 0.005

[a] The results from previous simulations[17] for water−methanol mixtures are also listed.

systems with an explicit silica substrate show penetration for water−methanol solvent mixtures and chains in relatively extended conformations.[15,16] Furthermore, in our previous work probing the chain conformation in aqueous methanol solutions,[15,17] it was observed that an isolated *n*-octadecane chain prefers rather extended but not all-trans conformations over the entire concentration regime for water−methanol solvent mixtures. In contrast, simulation studies for more hydrophobic chains (with 22 or 25 segments, stronger dispersive segment−segment interactions, and/or less torsional rigidity) show a preference for folded structures.[18,19]

The purpose of this paper is to extend our computational study on the solvation of *n*-octadecane to water−acetonitrile mixtures. In particular, we focus on the chain conformation and the local solvent environment to elucidate the difference between alkane/water−methanol and alkane/water−acetonitrile interactions.

II. Molecular Models and Simulation Details

The simulation setup is very similar to our previous study on water−methanol solvation.[17] It consists of a single *n*-octadecane chain solvated either in water−acetonitrile solutions with an acetonitrile mole fraction of 33% or 67% (systems 33A and 67A, respectively) or in neat acetonitrile (system ACN). All three systems contained 900 solvent molecules (see Table 1), and the simulations were carried out at a temperature of 323.15 K and at a pressure of 1015 kPa (10 atm).

The united-atom version of the transferable potentials for phase equilibria (TraPPE-UA) force field[20−22] was used for *n*-octadecane and acetonitrile, and water was represented by the TIP4P model.[23] The Lennard-Jones parameters for unlike interactions were determined from the Lorentz−Berthelot combining rules.[24] A site−site-based, spherical cutoff at 14.0 Å and analytical tail corrections[25] were used for the Lennard-Jones interactions, and the Ewald summation technique[25] was employed to compute the Coulombic interactions arising from the partial charges on the acetonitrile and water molecules.

Monte Carlo simulations for the three systems were carried out in the isobaric−isothermal ensemble.[26] In addition to the usual translational[27] and rotational displacements[28] and volume moves,[26] the conformational degrees of freedom of the *n*-octadecane chain were sampled using a combination of coupled−decoupled configurational-bias Monte Carlo (CBMC) moves for regrowing multiple segments including at least one terminal group[29−31] and self-adapting fixed-endpoint CBMC moves for regrowing multiple interior segments.[32]

For each of the systems, four independent simulations were carried out, and the standard deviations were estimated from the results of these independent simulations. The production periods consisted of up to 270 000 Monte Carlo cycles where one cycle involves N randomly selected moves, where N (= 901) is the total number of molecules. The statistical uncertainties listed in the tables and shown in the figures are the standard errors of the mean computed from the four independent simulations.

III. Results and Discussion

A. Conformation of Chains in Different Environments. Figure 1 shows the evolution of the end-to-end distance, r_E, for the solvated *n*-octadecane chain. For all solvent environments, one can observe that the alkyl chain mostly undergoes minor fluctuations around $r_E \approx 17$ Å. Occasionally, rapid transitions from this relatively extended state to a more collapsed state with $r_E \approx 5$ Å are observed, but the chain conformation does not remain in the collapsed state for extended periods.

In order to compare the results for the whole concentration range of water−acetonitrile mixtures, data from our simulations using neat water as the solvent (system WAT)[17] are also included in the following discussion. The probability distribution of the end-to-end distances of the solvated *n*-octadecane chains averaged over the four independent simulations are compared in Figure 2. A bin width of 2 Å was used for this analysis. Similar as for solvation in water−methanol mixtures,[17] the main peak appears at 17 Å and is highly asymmetric with an extended tail toward a shorter end-to-end distance. The minor peaks at 5 Å correspond to a folded state. For system WAT, the main peak is somewhat sharper and the minor peak is more pronounced than for the three water−acetonitrile systems (33A, 67A, and ACN). The average end-to-end distances, $\langle r_E \rangle$, are listed in Table 1. For the water-rich solvent environments (WAT, 33A, and also 33M[17]), $\langle r_E \rangle$ falls close to 14.5 Å, whereas the organic-rich phases (67A, ACN, and also 67M and MET[17]) yield a slightly larger value of about 15.6 Å.

The folding equilibrium constants, K_{UN},[17] between extended (unfolded) states (with $r_E > 8$ Å) and collapsed (native) states (with $r_E \leq 8$ Å) are listed in Table 1. The values for K_{UN} range from 0.03 (for systems 67A and ACN)

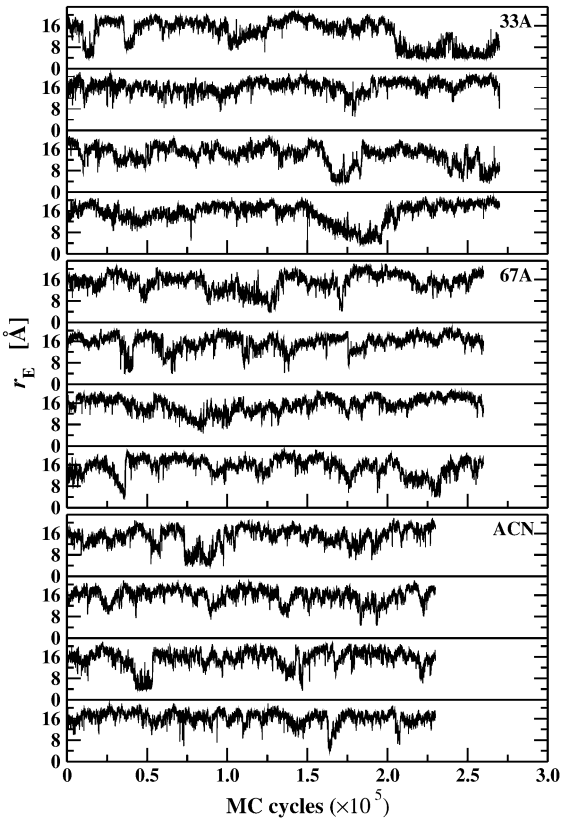

Figure 1. Evolution of the end-to-end distance of the solvated *n*-octadecane chains. Data are shown separately for the four independent simulations for each system: 33A (top), 67A (middle), and ACN (bottom).

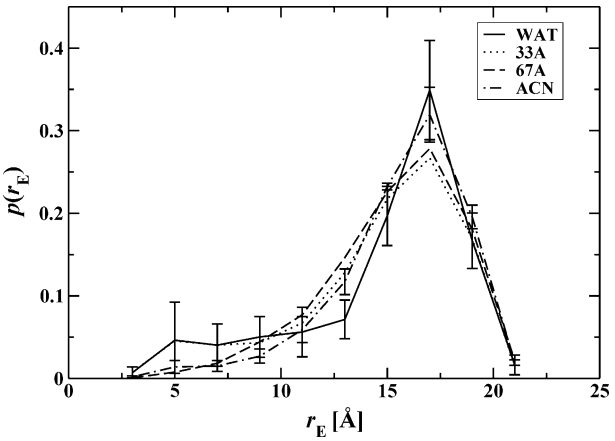

Figure 2. Probability density of the end-to-end distance for *n*-octadecane in four different environments. The solid, dotted, dashed, and dashed-dotted lines show the data for solvation in WAT, 33A, 67A, and ACN, respectively. For clarity, the standard errors of the mean are only shown for systems WAT and ACN.

to about 0.1 (for systems 33A and WAT), that is, in all solvent environments investigated here (and also for water−methanol mixtures);[17] extended states are strongly preferred, but folded states are sampled with significantly higher frequency in the water-rich environments. A comparison between the values for water−methanol solutions and those for water−acetonitrile solutions shows that the K_{UN} values are quite similar in the water-rich solvent environment

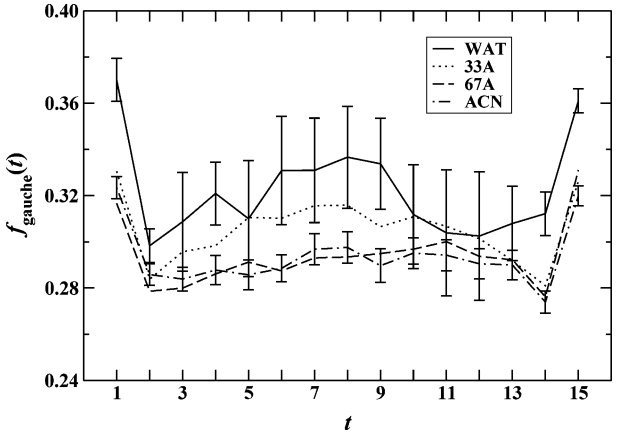

Figure 3. Fraction of gauche defects along the carbon backbone. Line styles are as in Figure 2.

(WAT, 33A and 33M) and very close in the organic-rich environment (67A, ACN, and 67M). Except for MET, the K_{UN} is smaller; that is, more extended conformations exist in the MET system.

Figure 3 depicts the fraction of gauche defects as a function of the position along the chain backbone. For all four solvents, the overall gauche fractions fall well-below 36%, the value that would be expected on the basis of a Boltzmann population analysis of the torsional potential for an ideal chain at the same temperature.[17,33] This shows that steric hindrance is more important than chain segment−segment attraction and solvent-induced forces that might favor folded states with more gauche defects than for an ideal chain. Only the terminal dihedral angles in system WAT have a gauche fraction of about 36%. Comparing the different solvation environments, one can see that, as the concentration of acetonitrile increases, the fraction of gauche defects decreases, though the difference is not dramatic. The *n*-octadecane chain in system WAT contains about 33% gauche defects, followed by that in system 33A with 31%, and then system 67A and 33M with about 29%. It is clear that the gauche defect distribution is related to the end-to-end distance distribution: chains that have higher probabilities in folded states also have a relatively higher fraction of gauche defects near the chain center. The reason for this is that gauche defects near the chain center are required to allow a chain to fold back on itself and bring the two chain ends into close contact.

B. Preferential Solvation. In order to investigate the local preferential solvation of the *n*-octadecane chain, radial distribution functions (RDFs), radial number densities (RNDs), and their corresponding number integrals (NIs) of solvent functional groups around the methyl or methylene groups of *n*-octadecane are compared in Figures 4 and 5. Compared with the local solvation environment found in water−methanol mixtures,[17] similar trends are observed for the RDFs and NIs between $CH_2/CH_3(C_{18})$ and ACN functional groups. The height of the first peak increases as the acetonitrile concentration decreases, while the NIs show that the number of ACN functional groups (N or CH3) increases with increasing concentration; that is, there is an enhancement in the composition but not in the absolute number of

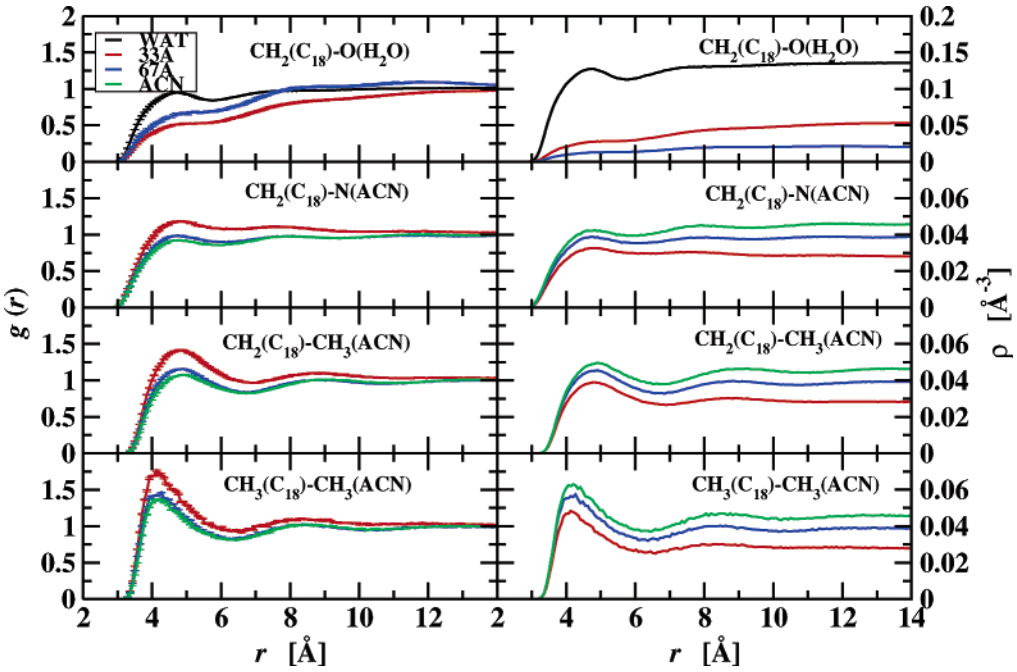

Figure 4. Radial distribution functions (left column) and radial number densities (right column) for solute segment−solvent segment pairs: top row, $CH_2(C_{18})$−$O(H_2O)$; second row, $CH_2(C_{18})$−N(ACN); third row, $CH_2(C_{18})$−CH_3(ACN); bottom row, $CH_3(C_{18})$−CH_3(ACN). The black, red, blue, and green lines represent WAT, 33A, 67A, and ACN systems, respectively.

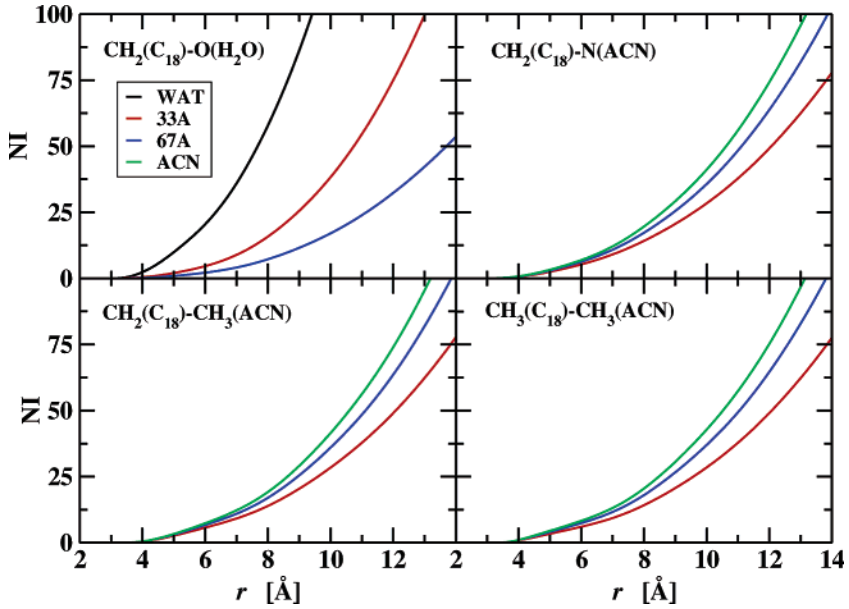

Figure 5. Number integrals for solute segment−solvent segment pairs: top left, $CH_2(C_{18})$−$O(H_2O)$; top right, $CH_2(C_{18})$−N(ACN); bottom left, $CH_2(C_{18})$−CH_3(ACN); bottom right, $CH_3(C_{18})$−CH_3(ACN). Line styles are as in Figure 4.

ACN molecules in the solvation shell. The first peak height in the RDFs for the $CH_2(C_{18})$−CH_3(ACN) pairs exceeds those for the $CH_2(C_{18})$−N(ACN) pair, but the difference is small compared to the corresponding RDFs involving the methyl group and oxygen atom of methanol.[17] Thus, the orientational distribution of the ACN molecules in the first solvation shell is more uniform than that for methanol, which has a clear preference for pointing with its methyl tail toward the chain.[17] Because of the larger accessible surface area and, hence, larger hydrophobicity of a methyl group compared to a methylene group, the local ACN structuring is further enhanced around the terminal methyl group of the C_{18} chain. Overall, the local solvation environment for the *n*-octadecane chain in systems ACN and 67A are quite similar, whereas that for system 33A differs substantially. This jump agrees with the folding equilibrium constants discussed above. Overall, it is apparent that, at typical chromatographic conditions, the organic modifier concentrations are sufficiently high that significant nonlinearities are observed for the RDFs, RNDs, and NIs of acetonitrile around the solute (i.e., RNDs and NIs do not show equal spacing). A similar observation was made for the mutual solubilities of ACN/water mixtures in *n*-hexadecane.[34] On the side, one may note that many experimental and simulation studies of bio-

Table 2. Numbers of Molecules, Mole Fractions, and Acceptor and Donor Hydrogen Bonds Per Molecule and Water's Tetrahedral Order Parameter Found in the Hydration Shell and Bulk Solvent

system	WAT	33A	67A	ACN
$N_{shell}(H_2O)$	90.0 ± 0.5	23.9 ± 0.6	10.9 ± 0.3	
N_{shell}(ACN)		26.2 ± 0.2	31.7 ± 0.1	35.7 ± 0.1
x_{shell}(ACN)		0.52 ± 0.01	0.74 ± 0.02	
$n^{acc}_{shell}(H_2O)$	1.80 ± 0.01	1.11 ± 0.01	0.69 ± 0.02	
n^{don}_{shell} (H_2O)	1.80 ± 0.01	1.78 ± 0.01	1.78 ± 0.01	
n^{acc}_{shell} (ACN)		0.84 ± 0.03	0.46 ± 0.01	
q_{shell} (H_2O)	0.13 ± 0.01	−0.46 ± 0.03	−0.47 ± 0.01	
x_{bulk} (ACN)		0.326 ± 0.001	0.668 ± 0.002	
n^{acc}_{bulk} (H_2O)	1.87 ± 0.01	1.33 ± 0.01	0.82 ± 0.01	
n^{don}_{bulk} (H_2O)	1.87 ± 0.01	1.8 ± 0.01	1.81 ± 0.01	
n^{acc}_{bulk} (ACN)		1.05 ± 0.01	0.50 ± 0.01	
q_{bulk} (H_2O)	0.477 ± 0.001	0.201 ± 0.001	0.038 ± 0.001	

molecule conformation and aggregation have shown linear behavior between bulk and vicinal concentrations at a low additive concentration.[35−37]

The $CH_2(C_{18})-O(H_2O)$ RDFs for both water−acetonitrile mixtures show a depletion of water near the C_{18} chain. However, as measured by the depressed height of the shoulder for the first solvation shell, the chain appears to be more dewetted for system 33A than for 67A. The opposite was observed for the water−methanol mixture; that is, the height of the peak/shoulder in the $CH_2(C_{18})-O(H_2O)$ RDFs decreased in the order WAT, 33M, to 67M.[17] On the other hand, the corresponding NIs (see Figure 5) show that, as the water concentration increases, the number of oxygen atoms (i.e., water molecules) around the chain segments increases from 67A to 33A. The unexpected order of the shoulder heights for the water−acetonitrile mixtures can be explained by the number of solvent molecules that, on average, populate the solvation shell. A simple distance-based criterion is used here to select solvent molecules as part of the first solvation shell; that is, a solvent molecule belongs to the solvation shell of *n*-octadecane if the separation between any solute segment and any heavy atom of the solvent molecule (including the methyl group and the nitrogen and α carbon atoms for acetonitrile and the oxygen atom for water) is less than 6 Å. The numerical values are listed in Table 2. The number of solvent molecules ranges from 90 for system WAT to 36 for system ACN, and the total numbers of solvent molecules for system 33A and 67A are 51 and 43, respectively. For both systems 33A and 67A, the solvation shells show enhanced acetonitrile mole fractions, which are 52% and 74%, respectively. It is clear that the enhancement by a factor of 1.6 for system 33A is much greater than that for system 67A, which is only 1.1. Therefore, the water concentration is much more depleted in system 33A, and even at this low concentration, the number of acetonitrile molecules in the first solvation shell has already reached about $^3/_4$ of the number found for neat acetonitrile. In contrast, for the water−methanol systems, the mole fractions of methanol in the first solvation shell are 46% and 76% for systems 33M and 67M, respectively.[17]

The local mole fraction enhancements[38] of solvent molecules around solute methyl or methylene groups for systems 33A and 67A are depicted in Figure 6. For both solvent

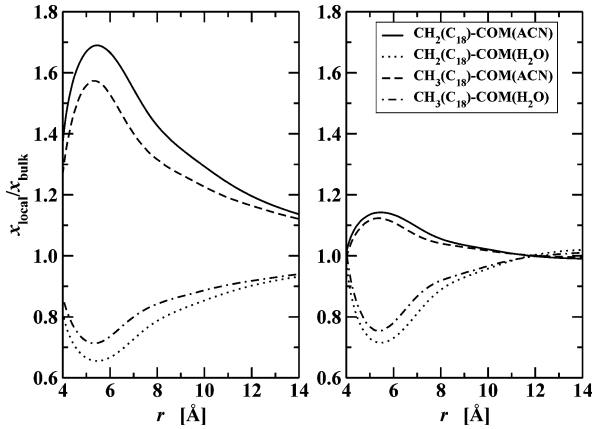

Figure 6. Local mole fraction enhancements in the vicinity of the *n*-octadecane chain for systems 33A (left) and 67A (right). The solid, dotted, dashed, and dotted−dashed lines represent $CH_2(C_{18})-COM(ACN)$, $CH_2(C_{18})-COM(H_2O)$, $CH_3(C_{18})-COM(ACN)$, and $CH_3(C_{18})-COM(H_2O)$, respectively.

mixtures, the local enhancement of acetonitrile peaks is at a separation of about 5.3 Å. The difference in molecular size is the reason for the lower enhancement at even smaller separation; that is, the smaller water molecule can approach somewhat closer than the larger acetonitrile molecule, but the number of solvent molecules at distances less than 4.5 Å is very small. We also should note a difference in the behavior of the local mole fraction enhancements between the water−acetonitrile and the water−methanol solvent mixtures. For the latter, the mole fraction enhancement is more pronounced around the methylene group, while the opposite is true for the water−acetonitrile mixture. The likely reason is that the large, linear acetonitrile molecule is not able to pack very well around the high-curvature contact surface of the methyl group.

C. Hydrogen-Bonding around the Solute. Hydrogen bonding around a nonpolar solute is also a topic of considerable interest.[18,19,39−41] Chandler and co-workers have pointed out that the disruption of the hydrogen-bonding network by a hydrophobic solute is scale-dependent. When the hydrophobic species is small, then the hydrogen-bonding network can persist, whereas the network is significantly disrupted

near large solutes (on the scale of nanometers).[40] More recently, Rajamani et al. have shown that the crossover length from small to large solute solvation is reduced by the addition of additives that lower the surface tension.[41] In Table 2, the numbers of hydrogen-bond donors and acceptors are compared for the solvation shell and the bulk solvent region. Here, any solvent molecule that is at least 12 Å away from any solute segment is considered to be in the bulk region (i.e., there is a 6-Å-thick buffer region between the shell and solvent). After checking that the geometric and energetic distributions are rather similar for hydrogen bonds involving oxygen or nitrogen as the acceptor, we continue to use the same hydrogen-bonding criteria as those for water/alcohol mixtures:[42,43] $r_{OX} \leq 3.3$ Å (where X can be the oxygen atom belonging to a second water molecule or the polar nitrogen atom), $r_{O\cdots H} \leq 2.5$ Å, $\cos\theta_{O-H\cdots X} \leq -0.1$, and $U_{pair} \leq -13$ kJ/mol, where $\theta_{O-H\cdots X}$ and U_{pair} are the hydrogen-bond angle and the interaction energy for a pair of solvent molecules, respectively. Because the methyl group in acetonitrile is modeled as a united atom, there cannot be a "weak" hydrogen bond involving a methyl hydrogen as the donor. Such interactions between a methyl hydrogen and a water oxygen were observed in a previous simulation study.[9]

For system WAT, it can be seen that the number of hydrogen bonds is about 4% higher for molecules belonging to the bulk region than that for molecules belonging to the solvation shell; that is, there is a minor disruption of the hydrogen-bond network. The fact that acetonitrile can only act as a hydrogen-bond acceptor leads to a donor−acceptor imbalance for the solvent mixtures. As a result, the number of hydrogen bonds accepted by a water molecule decreases in the order WAT, 33A, to 67A, with the decrease being more pronounced for the solvation shell than for the bulk region because of the acetonitrile mole fraction enhancement for the latter.

As discussed in a previous section, an acetonitrile molecule can only serve as a hydrogen-bond acceptor, a methanol molecule can serve as one donor and two acceptors, and a water molecule can contribute as two donors and two acceptors. Therefore, from Table 2, one can see that water molecules are involved in a higher number of hydrogen bonds as donors than as acceptors. Compared to systems 33M and 67M,[16] water molecules in systems 33A and 67A are involved in lower numbers of hydrogen bonds as acceptors. The number of acetonitrile molecules as acceptors is also lower than that for methanol molecules. It is also shown in Table 2 that, in the solvation shell, the number of molecules involved in hydrogen bonds is lower than that in the bulk. This difference is larger than in water−methanol systems. For acceptors (either water or acetonitrile), the average decrease is about 15%, while for donors, the decrease is only 2%. This could be due to the greater enrichment of acetonitrile in the solvation shell. Although the total number of hydrogen bonds donated by water molecules in the solvation shell decreases by only 1% from system WAT to 67A, there is a larger decrease for those water molecules in the bulk region; that is, the presence of acetonitrile leads to a disruption of the hydrogen-bond network in the bulk region of these systems.

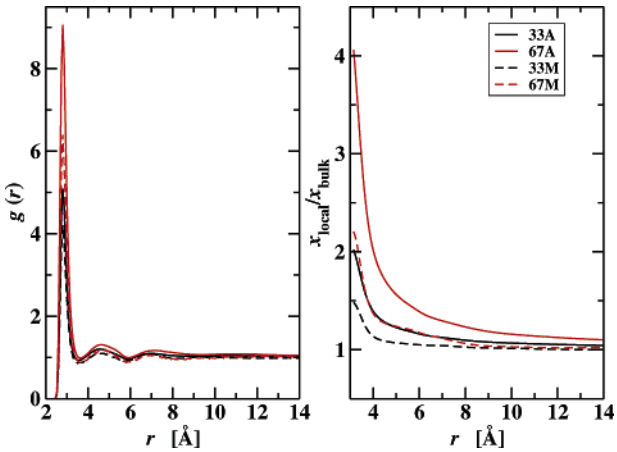

Figure 7. $O(H_2O)-O(H_2O)$ radial distribution functions (left) and local mole fraction enhancement for water (right). The black solid, red solid, black dashed, and red dashed lines depict data for systems 33A, 67A, 33M, and 67M, respectively.

D. Water Structure. As mentioned in the Introduction, it is well-known that water−acetonitrile mixtures show composition heterogeneities on small length scales, such as the preferential aggregation of water molecules.[9,10] The height of the first peak in the $O(H_2O)-O(H_2O)$ RDFs (see Figure 7) is significantly enhanced, with the enhancement being stronger for lower water concentration (systems 67A and 67M) and being stronger for water−acetonitrile mixtures than for water−methanol mixtures. A similar observation can also be made on the basis of the local mole fraction enhancement (see Figure 7). Although the composition enhancement is unambiguous, one should use care when interpreting the strong first peak in the $O(H_2O)-O(H_2O)$ RDF (e.g., with a value of about 9 for system 67A) as more structured water. Once the first peak in the RDF is divided by the local mole fraction enhancement at $r = 2.8$ Å, then the composition adjusted peak heights are 2.25, 2.55, 2.89, and 2.85 for systems 67A, 33A, 67M, and 33M. These rescaled peak heights for the water−methanol mixtures yield a value very close to that found for neat water, whereas those for the water−acetonitrile mixtures clearly fall below that for neat water.

A similar picture is also obtained by computing the tetrahedral order parameter for water.[44] Here, the nitrogen atom of acetonitrile is included in the search for the coordination shell. As can be seen from the data listed in Table 2, the tetrahedral order is significantly disrupted by the presence of acetonitrile. Thus, the composition enhancement for water goes hand-in-hand with a structural disordering.

IV. Conclusions

This computational study of a single *n*-octadecane chain solvated in water, acetonitrile, and their mixtures is an extension of our previous study in water−methanol systems. Simulation results show statistically significant but not dramatic differences in chain conformation. In all cases, including the water−methanol mixtures, the chain prefers unfolded conformations and the distribution of end-to-end distances peaks at 17 Å, a value that falls about 20% below

the end-to-end distance for the all-trans conformation. For both organic modifiers, the average end-to-end distance increases and the folding equilibrium constant decreases as the concentration of the organic modifier is increased.

The enhancement of acetonitrile with a concomitant depletion of water around the *n*-octadecane chain shows a different behavior as that in water−methanol mixtures due to the different hydrogen-bonding nature of the organic modifier. At a low organic concentration, water is significantly more depleted in system 33A than in 33M, and the concentration enhancement for acetonitrile extends to larger distances than that for methanol. However, acetonitrile does not pack well near methyl groups, and the enhancement of the acetonitrile mole fraction is more pronounced near methylene groups, whereas the opposite is true for methanol. Although water−water contacts are enhanced in water−acetonitrile mixtures compared to water−methanol mixtures, the presence of acetonitrile is more disruptive for water's tetrahedral hydrogen-bonding network. Overall, it appears that, for a given mole fraction, acetonitrile causes more significant changes than methanol in the solubility characteristics of aqueous solutions, which agrees with chromatographic observations.[3−8]

Acknowledgment. Financial support from the National Science Foundation (CHE-0213387) and the Advanced Biosciences Division of the Rohm and Haas Company is gratefully acknowledged. Part of the computer resources were provided by the Minnesota Supercomputing Institute.

References

(1) Przybyciel, M.; Majors, R. E. Phase Collapse in Reversed-Phase Liquid Chromatography. *LCGC North Am.* **2002**, *20*, 516.

(2) Walter, T. H.; Iraneta, P.; Capparella, M. Mechanism of retention loss when C8 and C18 HPLC columns are used with highly aqueous mobile phases. *J. Chromatogr., A* **2005**, *1075*, 177.

(3) Alvarez-Zeeda, A.; Barman, B. N.; Martire, D. E. Thermodynamic Study of the Marked Differences between Acetonitrile/Water and Methanol/Water Mobile-Phase Systems in Reversed-Phase Liquid Chromatography. *Anal. Chem.* **1992**, *64*, 1978.

(4) Guillaume, Y. C.; Gunichard, C. Retention Mechanism of Weak Polar Solutes in Reversed-Phase Liquid Chromatography. *Anal. Chem.* **1996**, *68*, 2869.

(5) Stalcup, A. M.; Martire, D. E.; Wise, S. A. Thermodynamic Comparison of Monomeric and Polymeric C_{18} Phases Using Aqueous Methanol and Acetonitrile Phases. *J. Chromatogr., A* **1988**, *442*, 1.

(6) Balakrishnan, S.; Easteal, A. J. Intermolecular Interactions in Water + Acetonitrile Mixtures : Evidence from the Composition Variation of Solvent Polarity Parameters. *Aust. J. Chem.* **1981**, *34*, 943.

(7) Carr, P. W.; Doherty, R. M.; Kamlet, M. J.; Taft, R. W.; Melander, W.; Horvath, C. Study of Temperature and Mobile-Phase Effects in Reversed-Phase High-Performance Liquid Chromatography by the Use of the Solvatochromic Comparison Method. *Anal. Chem.* **1986**, *58*, 2674.

(8) Kazakevich, Y. V.; LoBrutto, R.; Chan, F; Patel, T. Interpretation of the Excess Adsorption Isotherms of Organic Eluent Components on the Surface of Reversed-Phase Adsorbents Effect on the Analyte Retention. *J. Chromatogr., A* **913**, *2001*, 75.

(9) Kovacs, H.; Laaksonen, A. Molecular Dynamics Simulation and NMR Study of Water−Acetonitrile Mixtures. *J. Am. Chem. Soc.* **1991**, *113*, 5596.

(10) Mountain, R. D. Molecular Dynamics Study of Water−Acetonitrile Mixtures. *J. Phys. Chem. A* **1999**, *103*, 10744.

(11) Mountain, R. D. Molecular Dynamics Study of Thin Water−Acetonitrile Films. *J. Phys. Chem. B* **2001**, *105*, 6556.

(12) Satoh, Y; Nakanishi, K. Theoretical Studies of Acetonitrile−Water Mixtures/Monte Carlo Simulation. *Fluid Phase Equilib.* **1995**, *104*, 41.

(13) Klatte, S. J.; Beck, T. L. Microscopic Simulation of Solute Transfer in Reversed Phase Liquid Chromatography. *J. Phys. Chem.* **1996**, *100*, 5931.

(14) Slusher, J. T.; Mountain, R. D. A Molecular Dynamics Study of a Reversed-Phase Liquid Chromatography Model. *J. Phys. Chem. B* **1999**, *103*, 1354.

(15) Zhang, L.; Sun, L.; Siepmann, J. I.; Schure, M. R. A Moleculer Simulation Study of the Bonded-Phase Structure in Reversed-Phase Liquid Chromatography with Neat Aqueous Solvent. *J. Chromatogr., A* **2005**, *1079*, 127.

(16) Zhang, L.; Rafferty, J. L.; Siepmann, J. I.; Schure, M. R. A Moleculer Simulation Study of the Bonded-Phase Structure in Reversed-Phase Liquid Chromatography with Neat Aqueous Solvent. *J. Chromatogr., A* **2006**, *1126*, 219.

(17) Sun, L.; Siepmann, J. I.; Schure, M. R. Conformation and Solvation Structure for an Isolated *n*-Octadecane Chain in Water, Methanol, and Their Mixtures. *J. Phys. Chem. B* **2006**, *110*, 10519.

(18) Mountain, R. D.; Thirumulai, D. Molecular Dynamics Simulations of End-to-End Contact Formation in Hydrocarbon Chains in Water and Aqueous Urea Solution. *J. Am. Chem. Soc.* **2003**, *125*, 1950.

(19) Ghosh, T.; Kalra, A.; Garde, S. On the Salt-Induced Stabilization of Pair and Many-Body Hydrophobic Interactions. *J. Phys. Chem. B* **2005**, *109*, 642.

(20) Martin, M. G.; Siepmann, J. I. Transferable Potentials for Phase Equilibria. 1. United-Atom Description of *n*-Alkanes. *J. Phys. Chem. B* **1998**, *102*, 2569.

(21) Wick, C. D.; Stubbs, J. M.; Rai, N.; Siepmann, J. I. Transferable Potentials for Phase Equilibria. 7. United-Atom Description for Nitrogen, Amines, Amides, Nitriles, Pyridine and Pyrimidine. *J. Phys. Chem. B* **2005**, *109*, 18974.

(22) Siepmann, J. I. TraPPE: Transferable Potentials for Phase Equilibria Force Field. http://www.chem.umn.edu/groups/siepmann/trappe/intro.php (accessed July 20, 2006).

(23) Jorgensen, W. L.; Chandrasekhar, J.; Madura, J. D.; Impey, R.; Klein, M. L. *J. Chem. Phys.* **1983**, *79*, 926.

(24) Maitland, G. C.; Rigby, M.; Smith, E. B.; Wakeham, W. A. *Intermolecular Forces: Their Origin and Determination*; Oxford University Press: Oxford, U. K., 1987; p. 155.

(25) Allen, M. P.; Tildesley, D. J. *Computer Simulation of Liquids*; Oxford University Press: Oxford, U. K., 1987; pp 65, 156ff.

(26) McDonald, I. R. *NpT*-Ensemble Monte Carlo Calculations for Binary Liquid Mixtures. *Mol. Phys.* **1972**, *23*, 41.

(27) Metropolis, N.; Rosenbluth, A. W.; Rosenbluth, M. N.; Teller, A. H.; Teller, E. Equation of State Calculations by Fast Computing Machines. *J. Chem. Phys.* **1953**, *21*, 1087.

(28) Barker, J. A.; Watts, R. O. Structure of Water: A Monte Carlo Calculation. *Chem. Phys. Lett.* **1969**, *3*, 144.

(29) Martin, M. G.; Siepmann, J. I. Novel Configurational-Bias Monte Carlo Method for Branched Molecules. Transferable Potentials for Phase Equilibria. 2. United-Atom Description for Branched Alkanes. *J. Phys. Chem. B* **1999**, *103*, 4508.

(30) Siepmann, J. I.; Frenkel, D. Configurational-Bias Monte Carlo - A New Sampling Scheme for Flexible Chains. *Mol. Phys.* **1992**, *75*, 59.

(31) Vlugt, T. J. H.; Martin, M. G.; Smit, B.; Siepmann, J. I. ; Krishna, R. Improving the Efficiency of the Configurational-Bias Monte Carlo Algorithm. *Mol. Phys.* **1998**, *94*, 727.

(32) Wick, C. D.; Siepmann, J. I. Self-Adapting Fixed-Endpoint Configurational-Bias Monte Carlo Method for the Regrowth of Interior Segments of Chain Molecules with Strong Intramolecular Interactions. *Macromolecules* **2000**, *33*, 7207.

(33) Jorgensen, W. L.; Madura, J. D.; Swenson, C. J. Optimized Intermolecular Potential Functions for Liquid Hydrocarbons. *J. Am. Chem. Soc.* **1984**, *106*, 6638.

(34) Sun, L.; Siepmann, J. I.; Schure, M. R. Monte Carlo Studies of Partitioning Between *n*-Hexadecane and Water−Acetonitrile Mixtures. *J. Phys. Chem. B*, Submitted for publication.

(35) Timasheff, S. N. Control of Protein Stability and Reaction by Weakly Interacting Cosolvents: The Simplicity of the Complicated. *Adv. Protein Chem.* **1998**, *51*, 355.

(36) Parsegian, V. A.; Rand, R. P.; Rau, D. C. Osmotic Stress, Crowding, Preferential Hydration, and Binding: A Comparison of Perspectives. *Proc. Natl. Acad. Sci. U.S.A.* **2000**, *97*, 3987.

(37) Kalra, A.; Tugcu, N.; Cramer, S. M.; Garde, S. Salting-In and Salting-Out of Hydrophobic Solutes in Aqueous Salt Solutions. *J. Phys. Chem. B* **2001**, *105*, 6380.

(38) Chen, B.; Potoff, J. J.; Siepmann, J. I. Monte Carlo Calculations for Alcohols and Their Mixtures with Alkanes. Transferable Potentials for Phase Equilibria. 5. United-Atom Description of Primary, Secondary, and Tertiary Alcohols. *J. Phys. Chem. B* **2001**, *105*, 3093.

(39) Huang, D. M.; Chandler, D. The Hydrophobic Effect and the Influence of Solute-Solvent Attractions. *J. Phys. Chem. B* **2002**, *106*, 2047.

(40) Lum, K.; Chandler, D.; Weeks, J. D. Hydrophobicity at Small and Large Length Scales. *J. Phys. Chem. B* **1999**, *103*, 4570.

(41) Rajamani, S.; Truskett, T. M.; Garde, S. Hydrophobic Hydration from Small to Large Lengthscales: Understanding and Manipulating the Crossover. *Proc. Natl. Acad. Sci. U.S.A.* **2005**, *102*, 9475.

(42) Stubbs, J. M.; Siepmann, J. I. Aggregation in Dilute Solutions of 1-Hexanol in *n*-Hexane: A Monte Carlo Simulation Study. *J. Phys. Chem. B* **2002**, *106*, 3968.

(43) Chen, B.; Siepmann, J. I. Microscopic Structure and Solvation in Dry and Wet Octanol. *J. Phys. Chem. B* **2006**, *110*, 3555.

(44) Errington J. R.; Debenedetti, P. G. Relationship between Structural Order and the Anomalies of Liquid Water. *Nature* **2001**, *409*, 318.

CT600239Z